JOURNAL OF GEOPHYSICAL RESEARCH, SPACE PHYSICS VOL. 75, NO. 28, OCTOBER 1, 1970

Electron Observations between the Inner Edge of the Plasma Sheet and the Plasmasphere

M. A. SCHIELD AND L. A. FRANK

Department of Physics and Astronomy
University of Iowa, Iowa City 52240

Observations of electron intensities over the energy range ~100 ev to 50 kev are presented for L values between 3 and 10 R_E (earth radii) near local midnight at low magnetic latitudes. These measurements were obtained over the period June 11 through July 23, 1966, with an array of electrostatic analyzers borne on the earth satellite Ogo 3. The earthward edge of the plasma sheet is characterized by severe decreases in electron energy densities with decreasing geocentric radial distance. These decreases have a distinct structure with fluxes of higher energy electrons decreasing further from the earth for the electron energy range ~700 ev to 20 kev. A trough of ~100-ev electrons with number densities of ~1(cm)$^{-3}$ is observed to fill the region between the earthward edge of the plasma sheet and the plasmasphere. The densities of electrons with energies greater than 700 ev are often less than 0.1 (cm)$^{-3}$ in this region. The observed separation between the inner edge of the plasma sheet and the plasmapause was ~1 to 3 R_E in June and ~3 to 5 R_E in July. Analysis of subsequent observations should determine whether this is a latitude or local time effect. The plasmapause is usually observed to be located at the minimum of the energy density profile for electrons with energies above 700 ev. At electron energies of ~200 ev a plasmapause structure comprising a sharp radially outward boundary and a broader inward boundary is observed. The observed lifetimes of ~10 days for lower energy electron ($E \sim 1$ kev) intensities in the plasmasphere that were enhanced during a moderate geomagnetic storm are similar to previously reported lifetimes for more energetic electron ($E \geq 500$ kev) intensities in the same region. Kilovolt electron intensities between the plasmasphere and the earthward edge of the plasma sheet decreased more rapidly and fell to typically quiescent values within the satellite's orbital period of 48 hours. Simultaneous observations of the angular distributions of electron intensities at two pitch angles in the plasma sheet revealed that these angular distributions approached isotropy for the several plasma sheet crossings that were examined. Differential energy spectrums of electron intensities for the plasma sheet, the earthward edge, the electron 'trough,' and the plasmasphere are also presented.

The plasma sheet is by its location and nature central to the problem of the origins of the auroras and the extraterrestrial ring currents. Although the plasma sheet was first observed about ten years ago, until recently difficulties with the development of suitable instrumentation for the measurements of low-energy charged particle intensities within the magnetosphere have hindered the acquisition of accurate and comprehensive measurements concerning the nature of the plasma sheet and its environs [*Gringauz*, 1969; *Frank*, 1967*a*, *b*]. *Vasyliunas* [1968] observed that the plasma sheet was characterized by a 'well-defined sharp inner-boundary.' Between 1700 and 2100 geocentric local time, this inner boundary was reported as being located at 11 (±1) R_E (earth radii) during geomagnetically quiescent periods. Typically, the electron energy density decreased exponentially inward at this earthward boundary with a scale length of about 0.4 R_E. During magnetic storms of the bay type this boundary moved earthward to geocentric radial distances ~6 to 8 R_E. *Frank* [1967*d*, 1968] observed that the earthward edge of the plasma sheet was located at increasing geocentric radial distances for higher electron energies between 1 and 10 kev. The near-earth decrease for fluxes of 2-kev electrons was about half an earth radius closer to the earth than the corresponding decrease for fluxes of 5-kev electrons. Our present purpose is to examine in greater detail the distributions of low-energy electrons in the region extending through the

earthward boundary of the plasma sheet into the plasmasphere at low magnetic latitudes near local midnight.

Instrumentation

Ogo 3 was launched on June 7, 1966, into a highly eccentric orbit with initial apogee and perigee geocentric radial distances of 20.1 R_E and 1.1 R_E, respectively, orbital inclination 30°, period 48.6 hours, and geocentric local time of the apogee position ~2200. The spacecraft attitude system provided a predetermined, monitored spacecraft orientation. However, this attitude control system suffered an electrical failure on July 23, 1966. All observations reported here were acquired before this failure. Figure 1 illustrates geomagnetic dipole latitude and geocentric local time as functions of geocentric radial distance for several representative passes. The angular range of the antisolar direction in geomagnetic latitude is also indicated. The local time range for these inbound passes from 10 to 5 R_E was 2120 to 0120.

The University of Iowa instrumentation utilizes four continuous-channel electron multipliers as particle detectors and four cylindrical-plate electrostatic analyzers for E/Q analyses of the energy spectrums. These analyzers were paired to measure, simultaneously and separately, the differential energy spectrums of proton and electron intensities over an energy range extending from ~100 ev to 50 kev. These two pairs of 'low energy proton and electron differential energy analyzers' were designated as Lepedea A and B and had orthogonal fields of view. The fields of view for Lepedea A were directed earthward, and those for Lepedea B were directed perpendicular to the fields of view of Lepedea A in the satellite-earth-sun plane. (See *Frank* [1967*a*] and the references

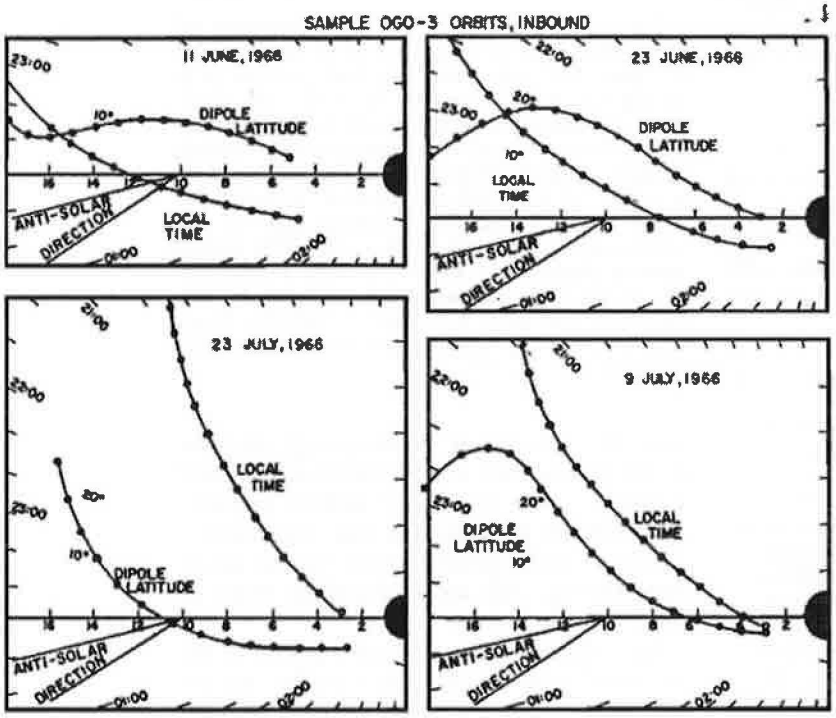

Fig. 1. Dipole magnetic latitude (solid circles) and geocentric local time (open circles) as functions of geocentric radial distance in units of earth radii for several representative inbound passes. The local times shift westward at the rate of ~1° per day. Although the spacecraft is at low dipole latitudes, with $\lambda_M \leq 25°$ within 15 R_E, the orbit cannot be described as near-equatorial beyond 8 R_E. An antisolar neutral sheet hinged to the dipole equatorial plane at 10 R_E would be within the indicated sectors.

therein for further details concerning the instrumentation.)

The energy bandpasses ('channels') for the two electron analyzers are summarized in Table 1. The analyzer plate voltages were stepped once every 19 sec, and the number of telemetered samples of intensities at each step, or bandpass, was dependent upon the spacecraft telemetry rate. A complete spectrum was acquired in approximately 5 min. The telemetered responses were corrected for background responses due to scattered electrons of higher energy whenever these background responses represented more than 10% of the detector count rate. Data are not presented for any period when the background responses are more than two-thirds of the detector count rate. Vertical arrows (Figure 2) are employed to designate observations for which the background responses were more than half of the telemetered detector count rate. Subsequent design improvements for later Lepedea systems derived from experience with this first analyzer array flow on Ogo 3 have greatly lessened these corrections for background responses attributable to solar ultraviolet and high-energy electrons on later spacecraft.

Observations

The next two following sections are directed toward detailed analysis of measurements of low-energy electron intensities for two observational periods, June 23 and July 17–21, 1966. These measurements display many of the features that are typical for low-energy electrons in the plasma sheet and its environs near local midnight during periods of relative magnetic quiescence. In subsequent sections observations for all available inbound passes for the period June through July are evaluated in terms of these exemplary passes.

TABLE 1. Energy Bandpasses for Ogo 3 Lepedea Electron Channels *A* and *B*

Electron Channel	Energy Bandpasses	
	A	*B*
3	90–160 ev	80–140ev
4	190–330 ev	170–300 ev
5	310–540 ev	280–500 ev
6	410–720 ev	380–680 ev
7	640–1100 ev	610–1100 ev
8	0.99–1.7 kev	0.94–1.7 kev
9	1.5–2.7 kev	1.5–2.7 kev
10	2.6–4.6 kev	2.8–5.0 kev
11	3.8–6.8 kev	4.1–7.2 kev
12	6.8–12 kev	5.8–10 kev
13	10–18 kev	9.8–17 kev
14	14–24 kev	14–24 kev
15	27–47 kev	26–46 kev

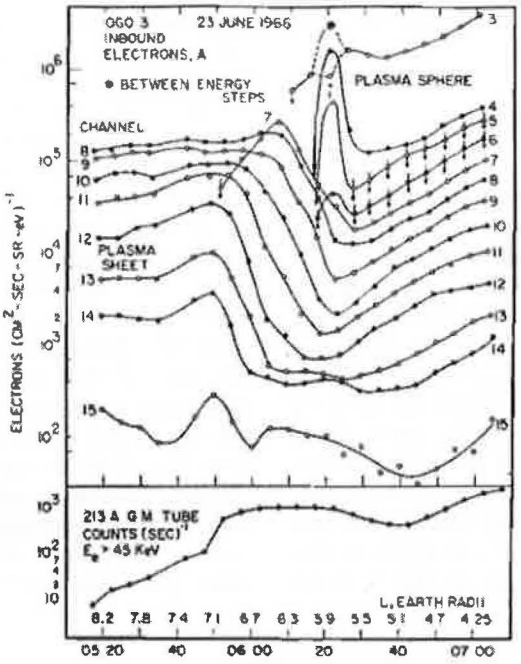

Fig. 2. Directional, differential intensities of electrons measured with Lepedea *A* as functions of time (UT) and magnetic shell parameter L during the inbound pass on June 23, 1966. Each curve is labelled with an energy bandpass number ('channel') and the corresponding energy ranges are tabulated in Table 1. The plasmapause is located at $L = 5.8$, the electron 'trough' is at $5.8 \lesssim L \lesssim 6.5$, and the earthward edge of the plasma sheet is at $5.8 \leq L \leq 7.1$. The simultaneous responses of a 213 GM tube to electron ($E > 40$ kev) intensities are included at the bottom of the figure. The familiar nightside 'trapping boundary' is evident in the sharp decrease of intensities at $L \simeq 7.0$.

June 23, 1966. The inbound segments of the spacecraft trajectory were positioned within one hour of local midnight at low magnetic latitudes as L decreased from 8 to 4 R_E. Figure 2 summarizes observations of the differential electron intensities as Ogo 3 passed through the inner edge of the plasma sheet and into the plasmasphere on June 23, 1966. Initially the fluxes of

electrons with energies above 10 kev (channels 12 and above) decreased with decreasing L value, while the fluxes of kilovolt electrons remained constant. Within a geocentric radial distance of 0.5 R_E, the fluxes of kilovolt electrons also began to decrease, and the peak fluxes shifted from channel 8 (990–1700 ev) to channel 7 (640–1100 ev). The decrease of electron (~10 kev) intensities with decreasing L values is evident over the L value range 7.1 to 6.1 (~1 R_E). This decrease of the higher energy electron intensities is coincident with an initial increase and subsequent decrease of 1-kev electron intensities (channel 7). At the near-earth termination of 10-kev electron intensities at $L \simeq 6.1$, there is a dramatic increase of lower energy ($E \lesssim 700$ ev) electron intensities (see channel 4, 190–330 ev; channel 5, 310–540 ev). The width of this maximum of lower energy electron intensities is ~0.5 R_E, and maximum intensities are closely positioned at the plasmapause. Inside the plasmasphere the differential intensities of electrons over the energy range 100 ev to 50 kev increased smoothly as the geocentric radial distance decreased. The simultaneous responses of a thin-windowed GM tube to electron ($E > 40$ kev) intensities are displayed at the bottom of Figure 2. It is difficult to infer any of the characteristics of the lower energy electron intensities with this familiar measurement of integral higher energy electron intensities. This relationship between the two measurements has been discussed previously by *Frank* [1967*a*, *d*].

The electron energy and number densities for the series of observations shown in Figure 2 are summarized as functions of magnetic shell parameter L in Figure 3. Two number and energy densities have been computed, corresponding to two energy ranges, 90 ev to 50 kev and 700 ev to 50 kev, to clarify the role of the lower energy electrons. For electron energies of 700 ev to 50 kev, the electron energy density decreased by a factor of 20 across the earthward edge of the plasma sheet. The corresponding decrease in electron number density was by approximately an order of magnitude. Although the electron intensities between 90 and 700 ev contributed negligibly to the energy density, these intensities were sufficiently large to maintain an essentially constant number density (90 ev to 50 kev) outside the plasmasphere. The region located between the earthward edge of the plasma sheet and the plasmapause at $5.8 \lesssim L \lesssim 6.5$ and

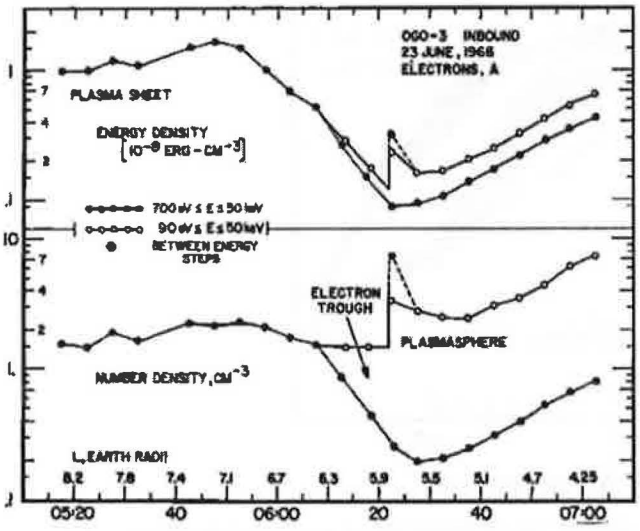

Fig. 3. Energy and number densities of electrons for two energy ranges 90 ev $\leq E \leq$ 50 kev (open circles) and 700 ev $\leq E \leq$ 50 kev (solid circles) as functions of time (UT) and shell parameter L corresponding to the series of observations shown in Figure 2. Across the earthward edge of the plasma sheet the electron energy densities decreased exponentially by an order of magnitude over $5.8 \leq L \leq 7.1$ with a scale length of 0.3 R_E. A constant number density of electrons with energies above 90 ev was maintained throughout the electron trough by the appearance of large intensities of lower energy electrons.

characterized by relatively large lower energy ($E \lesssim 700$ ev) electron intensities will be presently referred to as the 'electron trough.' As such this region is definitely a part of (but not necessarily identical with) *Carpenter's* [1966] 'plasma trough.' At the plasmapause both the number and energy densities of electrons (90 ev to 50 kev) were observed to increase abruptly (see Figure 3).

Sample differential energy spectrums of electron intensities for the observations presented in Figures 2 and 3 are shown in Figure 4. Within the plasma sheet these electron spectrums are relatively flat between 1 and 6 kev and decrease in intensities rapidly with increasing energies above 6 kev. If the directional differential intensities as functions of electron energy are approximated with the power law E^{-n}, then $n \simeq 0.5$ between 1 and 6 kev and $\simeq 2.7$ between 6 and 20 kev. Across the earthward edge of the plasma sheet the higher energy fluxes decrease initially (spectrum 2*a*), and then the kev electron intensities decrease with the appearance of larger 100-ev electron intensities (spectrum 2*b*), as the spacecraft moves to smaller geocentric radial distance. Within the plasmasphere, the energy spectrums are relatively smooth (i.e., intensities increase monotonically with decreasing electron energy), with $n \simeq 1.5$ for the energy range 300 ev to 50 kev, and $n \simeq 3.5$ for the differential spectrum for $E < 300$ ev. The locations, energy fluxes, and electron integral intensities for these spectrums are summarized in Table 2.

The radial gradients of lower energy electron intensities at the plasmapause on June 23 are indicated in the detailed presentation of detector responses of Figure 5. The time scale (abscissa) is referenced to time 0 sec at the beginning of channel 3 for Lepedea *A*. Each energy channel (numbered in Figure 5) is 19 sec in duration. The ordinate is detector response in counts (accumulation interval = 142 msec)$^{-1}$. The dotted circle indicates accumulation periods during which the plate voltages of the electrostatic analyzers were stepped. Four sets of

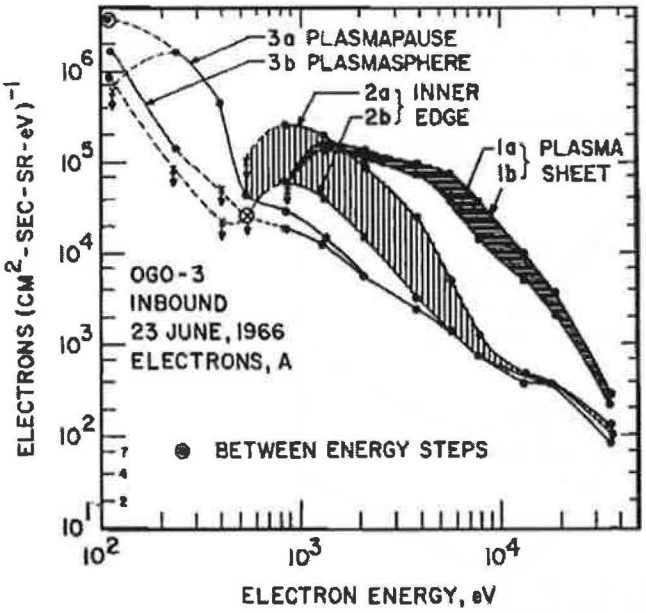

Fig. 4. Differential energy spectrums of electron intensities for the observations shown in Figure 2. The shading indicates that all spectrums acquired in a given region as noted in the figure lie between these minimum and maximum spectral intensities. Initially the higher energy intensities decreased between spectrums 1*b* and 2*a*, followed by a decrease in the kev intensities between spectrums 2*a* and 2*b*. Spectrum 2*b* illustrates the low-energy portion of the electron spectrums in the electron trough. The plasmapause differential intensities 3*a* quickly decrease to intensities similar to those for a typical plasmasphere spectrum 3*b*. The vertical arrows denote upper limits for differential intensities.

TABLE 2. Electron Energy Fluxes and Integral Directional Intensities

Spectrum	L, earth radii	Φ_E, ergs (cm² sec sr)⁻¹	J_e, (cm² sec sr)⁻¹
1*a*	8.2	5.6	6.3×10^8
1*b*	7.1	7.5	8.5×10^8
2*a*	6.4	1.8	4.5×10^8
2*b*	6.0	0.66	1.9×10^8
3*a*	5.8	0.62–0.64	$4.-6. \times 10^8$
3*b*	5.6	0.49	2.4×10^8

Data from Ogo 3, inbound, on July 23, 1966. 90 ev $\leq E \leq$ 50 kev.

responses to lower energy electrons at the plasmapause (see Figure 2) for each Lepedea *A* and *B* are shown in Figure 5; average responses at 0617 UT, all responses at 0622 UT and the average responses at 0627 UT (left side of Figure 5), and all responses at 0627 UT and the average responses at 0632 UT (right side). Comparison of the relative heights of the shaded areas that indicate differences in responses between these consecutive spectral measurements on the left (outward edge of the plasmapause) with those on the right (earthward, or inner, edge of the plasmapause) and reference to Figure 2 demonstrate that the increases of low-energy electron intensities at the outer edge of the plasmapause are more rapid than the subsequent decreases at the earthward edge. The position in time of the plasmapause is indicated in Figure 5 by the vertical dotted line at +18 sec (0622 UT spectrum). More specifically, the width of the outer edge is about 15 km (based upon a factor of 3 increase in count rate for channel 4*A*, in less than 5 sec at 0622:18 UT), assuming the plasmapause velocity is much less than the spacecraft's radial velocity of ~4 km (sec)$^{-1}$. Fifteen kilometers is the cyclotron radius for a 200-ev proton in the equatorial dipole field at 5.8 R_E. The inner edge has a thickness of between 200 km (based on the decline of channel 5*A* responses for the 0622 UT spectral measurement shown in Figure 5) and 1200 km (based upon the decline of channel 5*A* responses by the following 0627 UT spectral measurement). Even if the plasmapause were moving with a constant velocity, the ratio of the thickness of the inner and outer edges should be invariant. This ratio is between 20 and 120, which brackets the ratio of the cyclotron radii for protons and electrons with equal energies.

July 17–21. A second series of observations of low-energy electron intensities within the plasma sheet, electron trough and plasmasphere are summarized in Figure 6. The average elec-

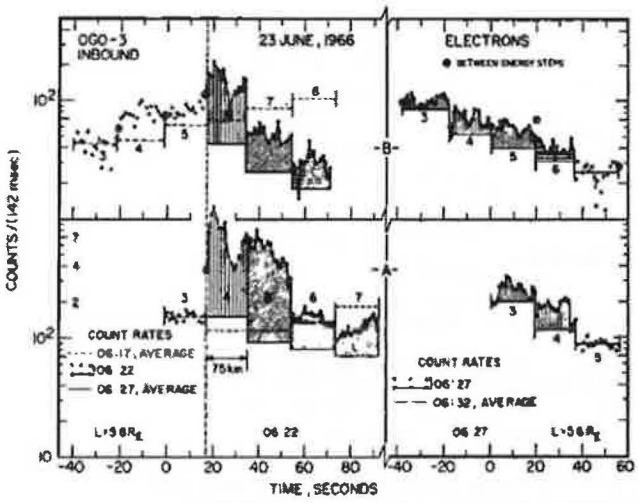

Fig. 5. Superposition of detailed responses of Lepedea *A* (lower half) and *B* (upper half) to lower energy electron intensities at the plasmapause crossing at $L = 5.8$ and 0622 UT (see Figure 2). The energy ranges corresponding to the numbered energy channels 3 through 8 are given in Table 1. The shaded areas represent the differences between the observed and the average count rates for the previous spectral measurement.

tron energy, energy density, and number density for the two energy ranges 750 ev to 50 kev and 90 ev to 50 kev are plotted as functions of magnetic shell parameter L for one segment each for the two inbound passes on July 21 (left side) and July 19 (right side). On July 21 at 1300 UT at $L \leq 7$, substorm-related phenomena not discussed in the present paper were observed. However, at $L \lesssim 8\ R_e$ the July 19 observations closely resemble the presubstorm measurements and are included in Figure 6 to provide the basic features of observations showing a different character relative to those of the previously discussed June 23 pass. Unlike the June 23 pass, the earthward edge of the plasma sheet is located several earth radii beyond the plasmapause, and the electron trough first appears at $L \simeq 9.5\ R_e$. The electron trough is easily identified by the sudden decrease in the average energy from ~2–5 kev to ~500–800 ev (rapid decrease in electron energy density and relatively small change in number density with decreasing L value). For electrons (90 ev $\leq E \leq$ 50 kev) the electron trough merges smoothly into the plasmasphere at $L = 5.65$.

Representative electron spectrums are displayed in Figure 7 for four regions within the magnetosphere near the magnetic equator and local midnight: plasma sheet, earthward edge of the plasma sheet, electron trough, and plasmasphere. These observations were obtained during the period July 17–19, 1966. The electron spectrum for the earthward edge of the plasma sheet features characteristics of both the plasma sheet spectrum and the electron trough spectrum. Although the trough spectrum resembles the plasmasphere spectrum, there appear to be significant differences. Below 300 ev the electron-trough spectrum ($n \simeq 2$) is harder than the plasmasphere spectrum ($n \simeq 3$). Furthermore, the electron-trough spectrum should peak in intensities near ~100 ev, while the plasmasphere spectrum should be characterized by a maximum in intensities below 30 ev if the total

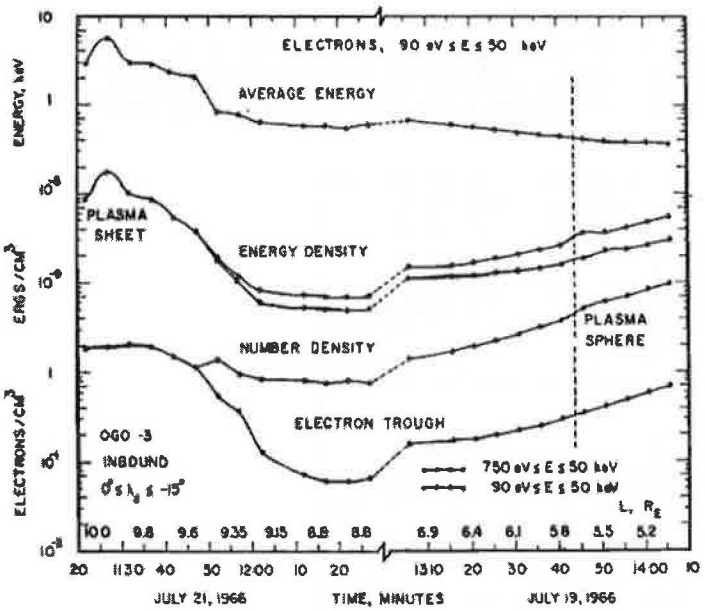

Fig. 6. Average electron (90 ev $\leq E \leq$ 50 kev) energy and energy densities and number densities as functions of time (UT) and L for two inbound passes on July 19 and July 21, 1966. The energy densities for electrons (90 ev $\leq E \leq$ 50 kev) and (750 ev $\leq E \leq$ 50 kev) are denoted by open and solid circles, respectively. The electron trough of ~100-ev electron intensities is easily discernible between the inner edge of the plasma sheet and plasmapause (see text). Unlike the June 23 observation, there is a smooth transition into the plasmasphere that may be associated with large intensities of higher energy electrons that were enhanced since the geomagnetic storm on July 9.

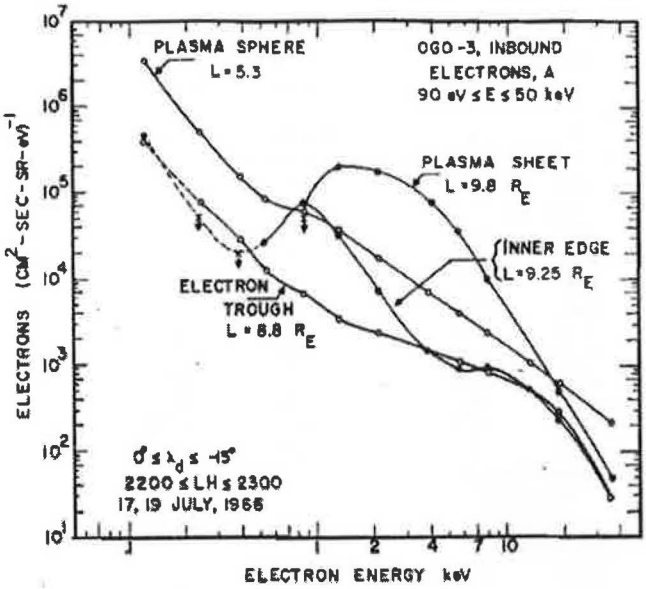

Fig. 7. Sample directional, differential spectrums of electron intensities for the plasma sheet, the earthward edge of the plasma sheet, the electron trough, and the plasmasphere for inbound passes on July 17 and 19.

electron densities of ~1 $(cm)^{-3}$ and ~100 $(cm)^{-3}$, respectively, observed by *Carpenter* [1966], are invoked. During this series of measurements the intensities within the electron trough increased steadily with decreasing L value to the position of the plasmapause where normally an abrupt increase in the electron (90 ev $\leq E \leq$ 50 kev) number density is observed. This effect may be related to the presence of relatively large intensities of higher energy electrons in the outer radiation zone during the poststorm period, following the July 9 geomagnetic storm.

Plasmapause identification. The results of a comparison of plasmapause locations utilizing simultaneous ion and electron observations are summarized in Table 3. The proton plasmapause observations are derived from measurements of ambient thermal ions between 1 and 45 atomic mass units, with a radio-frequency ion spectrometer on Ogo 3 [*Taylor et al.*, 1968]. The electron identification of the plasmapause position is most easily effected by identifying the localized enhancement of lower energy (~200 ev) electron intensities with those of the Lepedea's (channels 4). Electron and proton observations are typically within the 5-min temporal resolution of the Lepedea instrumentation.

Structure and location of the earthward edge of the plasma sheet. An abbreviated summary of the low-energy electron distributions observed for 22 consecutive inbound passes during the period June 11 through July 23, 1966, is attempted in Figures 8 and 9. Electron (90 ev $\leq E \leq$ 50 kev) energy densities as functions of L values from 3 to 10 R_E for each pass and positions of the plasmapause as identified from ion measurements, or electron measurements, or if the two observations of plasmapause position are coincident are included in Figure 9. The legend for the energy densities is given in Figure 8, with the designations for large flux decreases. Unless otherwise noted, these horizontal bars indicating rapid intensity decreases are for electron (990 $\leq E \leq$ 1700 ev) intensities (lower bar), and for electron (2.6 $\leq E \leq$ 4.6 kev) intensities (upper bar). These energy ranges correspond to channels 8 and 10, respectively (refer to Table 1). Intervals for which no reliable telemetry is available are indicated as dashed lines in Figure 9. D_{st} (H) as a function of time has been included at the left side of

TABLE 3. Comparison of Plasmapause Locations

Date	Protons* (Ion Detector) Time, UT	L, R_E	Electrons (Lepedea) Time, UT	L, R_E	Difference ΔT, minutes	ΔL, R_E
June 11	0220	7.04	~0220	7.0	0	0
June 15	0408	5.79	data gap			
June 17	0444	5.76	~0447	5.6	~3	0.15
June 19	0454	6.70	~0500	6.4	~6	0.3
June 21			0554	5.7		
June 23	0620	5.91	0622	5.9	2	0
June 25	0746	3.73	0748	3.6	2	0
June 27	0724	5.91	0727	5.9	3	0
June 29	0749	6.19	~0753	6.0	~4	0.2
July 1	0901	4.76	~0902	4.7	~1	0
July 3	0845	6.44	~0854	6.2	~9	0.25
July 5	0954	5.24	~0953	5.2	~1	0
July 7			unidentifiable†			
July 9	1156	3.31	unidentifiable			
July 11	1155	4.62	unidentifiable			
July 13	1139	6.20	unidentifiable			
July 15			~1245	5.3		
July 17	1310	5.63	~1310	5.6	0	0
July 19	1344	5.64	~1344	5.6	0	0
July 21	1432	5.18	missing frame			
July 23	1446	5.78	unidentifiable			

Data from Ogo 3, inbound.
* H. A. Taylor, personal communication, March 1969.
† Intense fluxes above 700 ev following a geomagnetic storm precluded a decisive observation.

Figure 9, where the periods corresponding to two moderate main-phase storms have been shaded. Since there is a large amount of information included in Figure 9 which also makes this figure somewhat difficult to cursorily examine, the following major features of the observed electron distributions are summarized here.

1. The two horizontal bars, upper and lower, designating the earthward edge of the plasma sheet, show the tendency for lower energy electron intensities (lower bar) to decrease closer to the earth relative to higher energy electron intensities (upper bar) during periods of relative magnetic quiescence. This structure has been shown in the detailed example of Figure 2.

2. The trough of lower energy electron intensities is invariably located in the region of low-energy density between the inner edge of the plasma sheet and the plasmapause.

3. The inward displacement of the plasmapause during main-phase geomagnetic storms is clearly evident.

4. The location of the earthward edge of the plasma sheet relative to the plasmapause is considerably different in July, relative to the location in June for magnetically quiet days. In June the separation between the plasmapause and the earthward edge of the plasma sheet is $\sim 1.5\ R_E$. In July this separation increases to ~ 3–$5\ R_E$, as the earthward edge of the plasma sheet withdraws to $\sim 8.5\ R_E$. This difference might be due to a latitude dependence resulting from the distortion of the distant geomagnetic field or a local time effect as the satellite trajectory moves into late evening. Analysis of further Ogo 3 observations should clarify this point.

5. During the moderate geomagnetic storm on June 25 the plasma sheet was first encountered at $L \simeq 9.3$ at $\lambda \simeq 20°$. The plasma sheet electrons penetrated to $4\ R_E$ with a peak energy density of $\sim 3 \times 10^{-4}$ ergs $(\text{cm})^{-3}$ and number density ~ 10–$30\ (\text{cm})^{-3}$ for the energy range 90 ev to 50 kev. The larger magnetic storm of July 9 is clearly evident by both the location and magnitudes of the electron energy

densities in Figure 9. This storm has been previously analyzed in detail by *Frank* [1967c]. On July 9 the total electron energy within the L shell range $1 \leq L \leq 8$ was $\sim 5 \times 10^{23}$ ergs, about a fourth of the proton total energy of 21×10^{23} ergs. These proton and electron energy reservoirs were shown to be possible explanations of the observed decrease of ~ 70 γ ($1\ \gamma = 10^{-5}$ gauss) at the earth's surface. Unlike the protons that have charge-exchange lifetimes of about one day at $L = 4$ [*Swisher and Frank*, 1968], the electron energy densities decay in an approximately exponential manner with a lifetime of ~ 10 days (see Figure 4 for the period July 9–23 at $L \simeq 4$). This observed lifetime for low-energy electrons ($1 \leq E \leq 50$ kev) is similar to that previously reported by *Roberts* [1969] for high-energy electrons ($E \geq 500$ kev) in the same region. Outside the plasmapause the enhanced electron energy densities were relatively quickly dissipated within a period of 2 days after the onset of the geomagnetic storm. These lifetimes are similar to those reported by *Craven* [1966] for electron ($E \geq 40$ kev) intensities on these L shells at low altitudes.

6. During a substorm observed to begin at 1300 UT on July 21 at College, Alaska, and which had just passed through the premidnight sector, the inner edge of the plasma sheet was encountered at $L = 9.7$. One hour later the electron energy density increased rapidly by a factor of 4 near $L = 6$. If this was indeed a second encounter with the inner edge of the plasma sheet, its average inward radial velocity must have exceeded 5.5 km sec^{-1} during that hour. An electric field of ~ 0.6 mvolt m^{-1} would drift plasma at this velocity in a 100-γ magnetic field. Further analysis of the simultaneous observations of low-energy proton intensities will be necessary to interpret this substorm behavior.

Discussion

Structure of the earthward edge of the plasma sheet. There are two types of theoretical explanations for the existence of the inner edge of the plasma sheet. Both are based upon a magnetospheric convective flow, as identified by *Axford and Hines* [1961], which carries charged particles toward the earth on the night side. These two groups of explanations are differentiated according to whether loss by atmospheric precipitation or loss by gradient drift is considered more essential to the formation of the earthward edge of the plasma sheet.

Loss by atmospheric precipitation was first investigated by *Petschek and Kennel* [1966], who proposed in an abstract that strong-diffusion precipitation would create a boundary for plasma sheet electrons at the location where the flow time and the minimum lifetime become comparable. An analysis of flow-precipitation coupling by *Kennel* [1969] indicated that in the midnight meridional plane the radial flow time and the electron precipitation time are comparable for auroral lines of force, and that higher energy particles should precipitate out at slightly greater radial distances. *Vasyliunas* [1966] speculated that resonant interactions with VLF waves would enhance electron precipitation. The resulting charge imbalance would induce a steady state electric field along the magnetic field lines, which would in turn draw up thermal ionospheric electrons to maintain charge neutrality. Such a mechanism would not necessarily affect the proton distributions and would be consistent with both a constant electron density across the earthward edge of the plasma sheet and the order of magnitude decreases in the 'temperature' of plasma sheet electrons at this position.

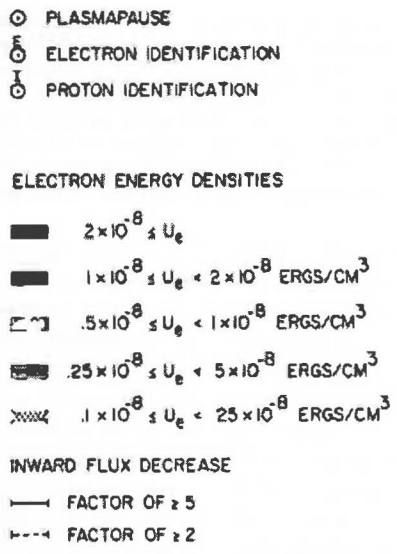

Fig. 8. Legend for the energy densities and symbols of the following Figure 9.

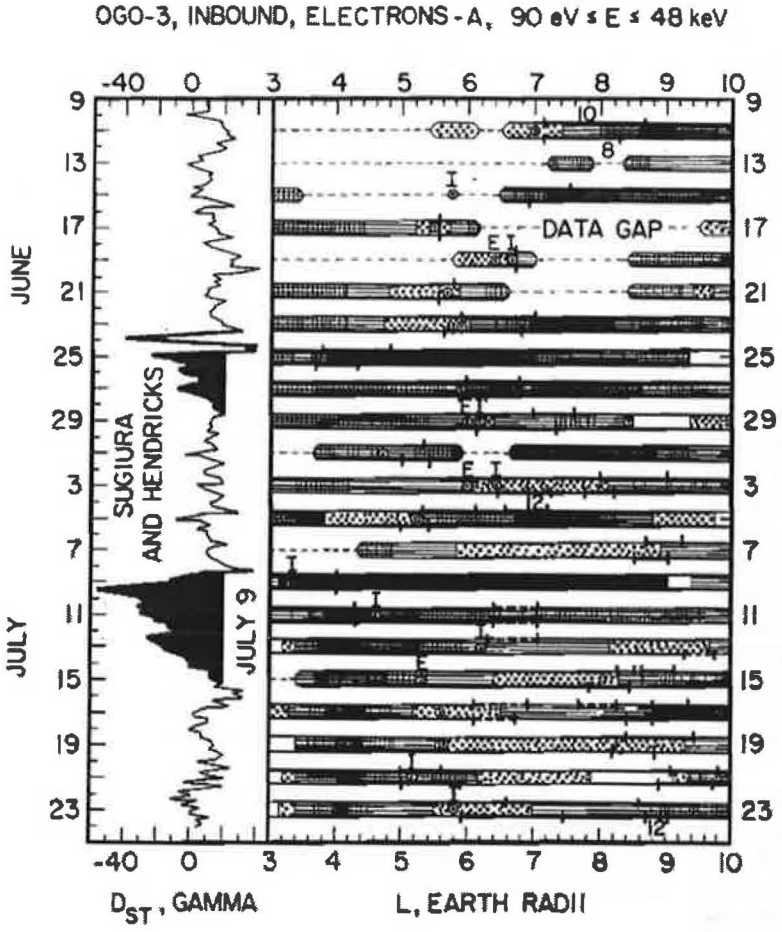

Fig. 9. Summary of electron (90 ev $\leq E \leq$ 48 kev) energy densities observed with Ogo 3 for 22 consecutive inbound passes as functions of magnetic shell parameter L over the range $3 \leq L \leq 10$ during June 11 through July 23, 1966. The plasmapause positions are indicated by dotted circle and (I) if the observation is by ion measurement only, by dotted circle and E if by electron measurement only, or by dotted circle alone if by coincident ion and electron measurements. D_{st}(H) for this period is displayed at the left side of the figure. The shaded portion of the D_{st}(H) profile indicates periods for two moderate geomagnetic storms. A summary of the important features of this graph appears in the text.

Loss by gradient drift was first evaluated by *Kavanagh et al.* [1968], who proposed that the earthward edge of the plasma sheet is an Alfvén layer. In this case the plasma sheet particles are convected into the dipolar geomagnetic field on the night side of the earth and are subsequently deflected azimuthally by enhanced gradient drift. This Alfvén mechanism would deflect higher energy particles at greater radial distances and would result in an inward decrease in the number density of the convected plasma-sheet particles. The charge separation arising from these motions could result in field-aligned currents that would be carried mainly by electrons with energies ~100 ev [*Schield et al.*, 1969; *Schield*, 1968]. The simultaneous deflection of convected protons would be moderated by the earth's corotational field, which allows energetic protons to penetrate more deeply into the magnetosphere than electrons with similar magnetic moments [*Schield*, 1969].

Loss by atmospheric precipitation and simultaneous loss by gradient drift have been examined by Vasyliunas, as discussed by *Kennel*

[1969]. By coupling strong-diffusion precipitation and gradient-drift modulated convective flow, Vasyliunas found that the sharp nightside temperature gradient extended from dusk through the late morning hours. In summary, although both loss processes are probably active, their relative importance remains to be evaluated.

One present observation, which is related to the interpretation of the earthward edge of the plasma sheet, concerns the pitch angle distribution of low-energy electron intensities at this position. Simultaneous measurements of the angular distributions of electron intensities at two pitch angles made with Lepedea *A* and *B* on June 11, 1966, are shown in Figure 10. The corresponding *dipole* pitch angles α for the fields of view of Lepedea *A* and *B* are ~(180°–65°) and ~35°, respectively. By definition pitch angle α is zero if the particle velocity is parallel to the magnetic field vector **B**. Any symmetric inflation of the dipole field should increase both α_A and α_B, thus decreasing the difference between the sines of their pitch angles. No significant dependence of the angular distributions of electron intensities upon radial distance is evidenced in the intensity profiles of Figure 10. This result was similar to that obtained for 6 inbound passes for which such an analysis was performed. However, it should be noted that the detector fields of view (8° × 30°) are larger than the local loss cone (half angle of several degrees) and that the fields of view were, with good probability, not directed into the loss cone. Hence this observation appears to be compatible with either of the above two loss mechanisms, since the explanation of loss by atmospheric precipitation assumes that pitch angle scattering is sufficiently strong to maintain isotropy over the loss cone, whereas the hypothesis of loss by gradient drift assumes that pitch angle scattering is neglible over time scales of a drift period. It should be noted, however, that there are no specific calculations presented in the literature and known to the authors that demonstrate that a mechanism of loss by gradient drift alone will produce an almost isotropic angular distribution such as that reported here.

Comparison with previous observations. In general, earlier observations of the charged

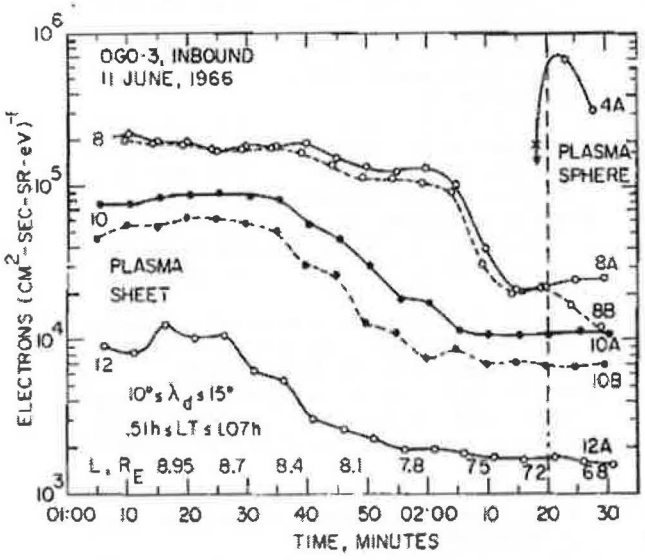

Fig. 10. Simultaneous observations of the angular distributions of electron intensities at two pitch angles with Lepedea *A* and *B* for the inbound pass on June 11, 1966. Directional, differential intensities are plotted as functions of time (UT) and *L*. The corresponding energy ranges for channels 4, 8, 10, and 12 are tabulated in Table 1. The *dipole* pitch angles viewed by Lepedea *A* and *B* are centered at ~(180°–65°) and ~35°, respectively, for this series of observations. On July 27 at $L = 3.6$, a cross-calibration of the two analyzers while viewing identical pitch angles verified that there was less than a 30% difference in the overall geometric factors of the two analyzers.

particle distributions within the plasma sheet are in fair agreement with those presented here. Peak integral electron intensities above 200 ev of $\sim 2 \times 10^{8}$ $(cm^2\ sec)^{-1}$ over approximately a hemisphere were measured with Lunik 1. The integral electron intensities of $\sim 10^{10}$ $(cm^2\ sec)^{-1}$ measured with Ogo 3 exceeded these by about an order of magnitude. *Freeman* [1964] noted that the electron flux would be $\sim 10^{9}$ $(cm^2\ sec\ sr)^{-1}$ if the observed energy flux were produced by 10-kev electrons. This equivalent energy flux of 16 ergs $(cm^2\ sec\ sr)^{-1}$ is within a factor of two of those presented here. The Ogo 3 measurements of the plasma sheet within 12 R_E indicate the average electron energy, $\hat{E} = (U_e/n_e)$, is ~ 3 to 5 kev, although the energy of the peak differential intensities occurs at ~ 1 kev.

The ATS low-energy detector observed particle fluxes of 3×10^{6} to 2×10^{7} $(cm^2\ sec\ sr)^{-1}$ at 6.6 R_E. Particles observed include electrons above 3 kev and all protons [*Freeman and Maguire*, 1967]. On June 23, 1966, inbound at $L = 6.6$ R_E at local midnight, Ogo 3 observations indicate that the integral electron intensity in the inner edge of the plasma sheet above 3 kev was 3.2×10^{8} $(cm^2\ sec\ sr)^{-1}$, a factor of 20 greater than the integral proton flux above 100 ev. Although the efficiencies of the ATS low-energy detector for both electrons and protons have not been published, *Frank* [1965] and *Frank et al.*, [1969] have shown that the electron multiplier efficiency for counting 3-kev electrons is $\sim 20\%$ to 40% of the efficiency for counting protons between 3 and 30 kev. Even so, on June 23 the electron flux would have produced at least 80% of the counts in such a detector. On July 19 at $L = 6.6$ R_E, the electron intensities in the electron trough above 3 kev were 2.8×10^{7} $(cm^2\ sec\ sr)^{-1}$, about 80% of the proton flux above 100 ev. In this environment the protons would produce at least 75% of the counts in such a detector. Even if the calibration of this instrumentation were available, the identification of the plasma component observed with the ATS low-energy detector above 50 ev in this environment would be difficult if not impossible.

Although *Vasyliunas'* [1968] main conclusions are corroborated here, his observation of the inner edge at 11 ± 1 R_E was not. The differences in the location of this inner edge may be entirely latitude and local time differences between the observations. Ogo 3 observations of the inner edge at $\lambda = 15°$ near local midnight could map onto an equatorial crossing radius of ~ 10 R_E. Furthermore, Vasyliunas' quiettime observations were made between 1700 and 2100 geocentric local time, whereas these Ogo 3 measurements were made between 2100 and 0100. Analyses of subsequent Ogo 3 data should clarify this difference.

Acknowledgments. We would like to thank H. A. Taylor of the Goddard Space Flight Center for generously providing plasmapause locations observed with his ion spectrometer.

This research was supported in part by the National Aeronautics and Space Administration under grant NGL-16-001-002 and contract NAS5-2054 and by the Office of Naval Research under contract Nonr-1509(06).

* * *

The Editor wishes to thank C. F. Kennel, V. M. Vasyliunas, and another referee for their assistance in evaluating this paper.

References

Axford, W. I., and C. O. Hines, A unifying theory of high-latitude geophysical phenomena and geomagnetic storms, *Can. J. Phys., 39*, 1433–1464, 1961.

Carpenter, D. L., Whistler studies of the plasmapause in the magnetosphere, *J. Geophys. Res., 71*, 693–709, 1966.

Craven, J. D., Temporal variations of electron intensities at low altitudes in the outer radiation zone as observed with satellite Injun 3, *J. Geophys. Res., 71*, 5643–5663, 1966.

Frank, L. A., Low-energy proton and electron experiment for the Orbiting Geophysical Observatories *B* and *E*, *U. Iowa Res. Rep. 65-22*, July, 1965.

Frank, L. A., Initial observations of low-energy electrons in the earth's magnetosphere with Ogo 3, *J. Geophys. Res., 72*, 185–195, 1967*a*.

Frank, L. A., Several observations of low-energy protons and electrons in the earth's magnetosphere with Ogo 3, *J. Geophys. Res., 72*, 1905–1916, 1967*b*.

Frank, L. A., On the extraterrestrial ring current during geomagnetic storms, *J. Geophys. Res., 72*, 3753–3767, 1967*c*.

Frank, L. A., Recent observations of low-energy charged particles in the earth's magnetosphere, in *Physics of the Magnetosphere*, edited by R. L. Carovillano, J. F. McClay, and H. R. Radoski, D. Reidel, Dordrecht, Holland, 1967*d*.

Frank, L. A., On the distribution of low-energy protons and electrons in the earth's magnetosphere, in *Earth's Particles and Fields*, edited by B. M. McCormac, Reinhold, New York, 1968.

Frank, L. A., N. K. Henderson, and R. L. Swisher, Degradation of continuous-channel electron multipliers in a laboratory operating environment, *Rev. Sci. Instrum., 40*, 685–689, 1969.

Freeman, J. W., Jr., The morphology of the electron distribution in the outer radiation zone and near the magnetospheric boundary as observed by Explorer 12, *J. Geophys. Res., 69*, 1691–1723, 1964.

Freeman, J. W., Jr., and J. J. Maguire, Gross local-time particle asymmetries at the synchronous orbit altitude, *J. Geophys. Res., 72*, 5257–5264, 1967.

Gringauz, K. A., Low energy plasma in the magnetosphere, *Rev. Geophys., 7*(1, 2), 339–378, 1969.

Kavanagh, L. D., Jr., J. W. Freeman, Jr., and A. J. Chen, Plasma flow in the magnetosphere, *J. Geophys. Res., 73*, 5511–5519, 1968.

Kennel, C. F., Consequences of a magnetospheric plasma, *Rev. Geophys., 7*(1, 2), 379–419, 1969.

Petschek, H. E., and C. F. Kennel, Tail flow, auroral precipitation and ring currents (abstract), *Trans. Amer. Geophys. Union, 47*, 137, 1966.

Roberts, C. S., Pitch-angle diffusion of electrons in the magnetosphere, *Rev. Geophys., 7*(1, 2), 305–337, 1969.

Schield, M. A., Configuration of geomagnetic field lines above the auroral zone, Ph.D. thesis, Rice University, Houston, Texas, 1968.

Schield, M. A., Drift of noninteracting charged particles in a simple geomagnetic field, *U. Iowa Res. Rep. 69-64*, 1969.

Schield, M. A., J. W. Freeman, and A. J. Dessler, A source for field-aligned currents at auroral latitudes, *J. Geophys. Res., 74*, 247–256, 1969.

Swisher, R. L., and L. A. Frank, Lifetimes for low-energy protons in the outer radiation zone, *J. Geophys. Res., 73*, 5665–5672, 1968.

Taylor, H. A., H. C. Brinton, and M. W. Pharo, III, Contraction of the plasmasphere during geomagnetically disturbed periods, *J. Geophys. Res., 73*, 961–968, 1968.

Vasyliunas, V. M., Observations of low energy electrons with the Ogo-A satellite, Ph.D. thesis, MIT, Cambridge, Mass., 1966.

Vasyliunas, V. M., A survey of low-energy electrons in the evening sector of the magnetosphere with Ogo 1 and Ogo 3, *J. Geophys. Res., 73*, 2839–2884, 1968.

(Received August 21, 1969;
revised June 3, 1970.)